Journal of Surgical Research **105,** 160–172 (2002)
doi:10.1006/jsre.2002.6372

A Novel Implantable Collagen Gel Assay for Fibroblast Traction and Proliferation during Wound Healing

Paul A. J. Enever,* David I. Shreiber,* and Robert T. Tranquillo*,†

**Department of Chemical Engineering and Materials Science and †Department of Biomedical Engineering, University of Minnesota, Minneapolis, Minnesota 55455*

Submitted for publication July 16, 2001; published online July 8, 2002

Background. **A novel implantable assay for studying cellular behavior in the wound environment was developed. The assay is unique in that it combines the more quantitative nature of *in vitro* assays with the greater physiological relevance of *in vivo* wound healing models.**

Materials and methods. **Cells were seeded in a physiologically relevant biological matrix, a collagen gel, contained within a semipermeable tube, and then exposed to soluble factors of the wound environment at different stages of the wound healing response. Gels were harvested at prescribed time points, and cell proliferation rates and gel compaction were measured. These data were combined with our theory for cell–matrix mechanical interactions to estimate the cell traction exerted by the cells leading to gel compaction. Cell morphology and α-smooth muscle actin expression were also characterized.**

Results. **The proliferation of and traction exerted by fibroblasts exposed to the soluble wound environment were different from those in similar collagen gels maintained in culture in complete medium. Proliferation and traction also varied over the course of the wound healing response. Traction was higher and proliferation lower in day 1–5 wounds compared to day 7–11 wounds. Recovered cells no longer stained for α-smooth muscle actin, in contrast to cells maintained in culture.**

Conclusions. **Changes in the soluble wound environment that occur as the wound healing response proceeds alter fibroblast traction and migration. We have developed a new assay that employs a physiologically relevant biological matrix and allows the effects of the dynamic soluble wound environment on cellular traction, proliferation, and other phenomena such as protein expression to be quantified.**

Key Words: **collagen gel; wound healing; wound contraction; fibroblast; cell traction; *in vivo*.**

INTRODUCTION

Wound healing comprises a complex interaction of cellular, biomechanical, and biochemical phenomena. Fibroblasts play a central role in wound healing by producing the extracellular matrix (ECM) molecules that ultimately replace the damaged tissue, by first migrating into the wound site and proliferating (fibroplasia) and then depositing new matrix and restructuring the tissue [1]. As part of the process of closure, wounds may undergo contraction, giving rise to scarring and loss of function [2, 3]. While the exact mechanism of wound contraction is still in dispute, it is now widely accepted that fibroblast traction provides the driving force [4].

Due to the complexity of the wound healing response, we have developed a number of *in vitro* assays that allow the quantitative measurement of selected cell behaviors important in wound healing. They all employ 3-D collagen or fibrin gels to provide a physiologically relevant experimental ECM. These include assays for chemotaxis [5, 6], contact guidance [7], traction [8, 9], and migration [8, 10]. We have recently used some of these assays to conduct a systematic investigation of the role of platelet-derived growth factor (PDGF) BB in modulating fibroblast traction and migration [11].

While *in vitro* collagen and fibrin gel assays provide a more physiologically relevant means of studying the role of growth factors such as PDGF BB in the wound healing response compared to monolayer cell culture on glass or plastic, they fail to capture several critical features of the wound. First, the assays are oversimplified in that they include interactions among a single combination of cell, ECM, and growth factor types. This shortcoming could be rectified by coculturing cells, using ECM mixtures, or adding multiple growth fac-

0022-4804/02 $35.00

tors, but such efforts would increase experimental complexity without necessarily providing a commensurate increase in biofidelity nor yielding greater insight into the wound healing process. Second, our assays are designed to provide fairly static conditions in contrast to the highly dynamic wound environment. Most notable is the continuous change in the composition of the soluble wound environment. For example, PDGF AA is present at elevated levels immediately after wounding that rapidly decline over the following 48 h [12]. While this change in composition could be mimicked by sequentially exposing *in vitro* gel assays to wound fluids from different postwound days, the result would be a discontinuous change in soluble wound mediator concentrations with increased potential for loss of growth factor activity under culture conditions.

A number of different *in vivo* models have been developed to study wound healing. These assays offer the advantage of an actual wound environment in contrast to the idealized one provided by *in vitro* systems. However, the ability to make quantitative measurements of cellular behavior is limited. Commonly, a model animal is wounded and some element of the repair process such as the rate of wound closure, the wound breaking strength, or the histology is observed [13–15]. Other models involve the implantation of some device in the wound site to act as a repository for wound fluid and as a structure onto which granulation tissue can form. These include the polyvinyl alcohol sponge [16, 17], the polyurethane sponge [18], the cellulose sponge [19–21], expanded polytetrafluoroethylene tubing [22, 23], the stainless steel wire mesh cylinder [24], and their variants. The implantable models are primarily useful for collecting wound fluid, monitoring inflammation, and studying fibroplasia and matrix deposition [25]. Only the nonimplant wound models provide any insight into wound contraction and then only if the wound boundary is fixed or has been marked, since contraction and matrix deposition can occur simultaneously. Further, these models provide no way to estimate cell traction from observed wound contraction since neither the cell density nor the tissue mechanical properties are precisely known. Finally, none of them permit fibroblasts to be exposed to soluble wound factors while interacting with a defined matrix that can be withdrawn and characterized at a later time.

An assay that combined the ability to quantify cell behavior and the soluble wound environment would be ideal. Herein, we present an assay in which a fibroblast-seeded collagen gel is enclosed in a semipermeable tube that is inserted into a sponge wound model and, thereby, exposed to the dynamic soluble wound environment. This assay precludes the ability to continuously monitor individual cells, but it does provide a means for estimating cell traction and measuring cell proliferation for cells exposed to the actual soluble wound environment.

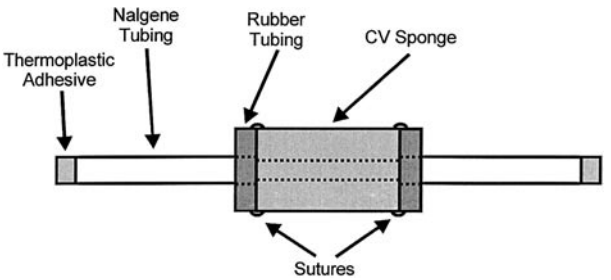

FIG. 1. Schematic of CV sponge assembly. Nalgene and rubber tubing is aligned concentrically with the core of the CV sponge and attached to the sponge with sutures. The tubing guides the PVDF membrane-enclosed collagen gel into the core of the CV sponge. Thermoplastic adhesive is used to seal the ends of the Nalgene tubing.

MATERIALS AND METHODS

Materials. Trypsin (25 mg/ml in 0.9% saline), ethylenediaminetetraacetic acid (EDTA), $CaCl_2$, NaOH, agarose, anti-α-smooth muscle actin monoclonal antibody, and TRITC-conjugated phalloidin were purchased from Sigma Chemical Co. (St. Louis, MO). Vitrogen 100 bovine type I collagen was from Cohesion Technologies, Inc. (Palo Alto, CA). Tissue culture medium, penicillin/streptomycin (pen–strep), Fungizone, Hepes buffer, phosphate-buffered saline (PBS), and L-glutamine were from Gibco Laboratories (Grand Island, NY). Fetal bovine serum (FBS) was from HyClone Laboratories (Logan, UT). Cored cylindrical cellulose vicose (CV) sponges were from Cellomeda (Turku, Finland). Nalgene PVC tubing was from Fisher Scientific (Pittsburgh, PA). Teflon thread was from McMaster-Carr (Chicago, IL). Sodium pentobarbitol was from Abbott Laboratories (Chicago, IL). Polyvinylidene difluoride (PVDF) dialysis membranes were from Spectrum Laboratories (Rancho Dominguez, CA). Propidium iodide and goat anti-mouse Alexa 488 antibody were from Molecular Probes (Eugene, OR).

Cell culture. Rat dermal fibroblasts (RDFs) were harvested from adult male Fisher rats using a primary explant technique [26] and kept in liquid nitrogen after slow freezing. Cell lines were initiated for culture by thawing an aliquot of cells and centrifuging at 1000 rpm for 10 min at 4°C. The pellet of cells was resuspended in Dulbecco's modified Eagle's medium (DMEM) supplemented with pen–strep (1% v/v) and L-glutamine (1% v/v). Cells were plated out on 60 × 15-mm petri dishes using 6 ml of DMEM with 10% FBS, 1% pen–strep, and 1% L-glutamine and kept in a humidified CO_2 incubator at 37°C. Trypsin/EDTA was used to pass the cells once a week at a 1:4 dilution. Cells were harvested with 0.5% trypsin/EDTA and washed twice with complete medium (Medium 199 containing Hanks' salts (M199) supplemented with 10% FBS, 1% pen–strep, and 1% L-glutamine). Cells were passed or harvested at 60–90% confluence. All experiments were conducted before the 10th passage, at which point a new culture was initiated from frozen cells.

Sponge wound model preparation. Cored CV sponges were placed in double-distilled water, allowed to swell, and then cut in half to yield two cylindrical cored sponges of approximately 2 cm in length. One-quarter-inch i.d. rubber tubing was cut into approximately 3-mm-thick cylindrical sections. Nalgene tubing of 3/16-in. i.d. × 1/4-in. o.d. dimension was cut into approximately 3.5-cm lengths. The rubber tubing was placed over one end of the Nalgene tubing and two sutures were used to attach one set of tubing to each end of a CV sponge as shown in Fig. 1. Teflon thread of 1/16 in. diameter was cut to 8.5-cm length and placed inside the sponge/tube assembly. The whole assembly was then placed in double-distilled water and auto-

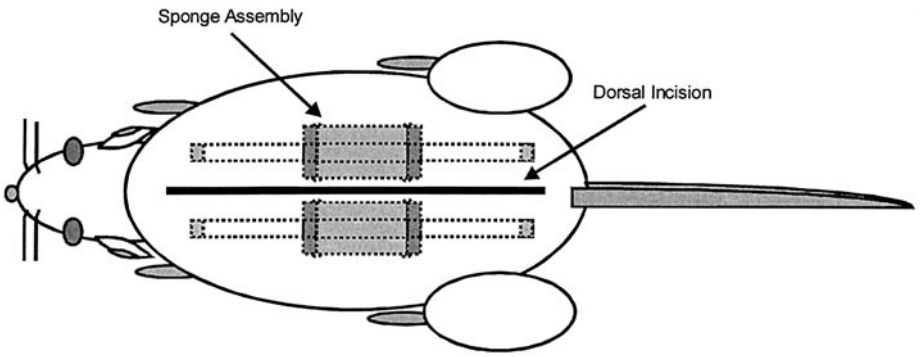

FIG. 2. Schematic of sponge assembly implanted in a rat. An incision is made in the dorsal side of the animal, and the skin on each side of the incision is separated from the underlying tissue. One sponge assembly is then placed under the skin on each side, and the incision is closed with surgical staples.

claved. Following sterilization, the open Nalgene tube ends were sealed with a thermoplastic adhesive, and the assembly was stored at 4°C in sterile water.

Sponge wound model implantation. All animal experiments were performed in accordance with the University of Minnesota's guidelines for the care and use of laboratory animals. Adult male Fisher rats were anesthetized with sodium pentobarbitol (50 mg/kg ip). The dorsal side of each animal was shaved and an approximately 12-cm-long incision was made. Blunt-nosed scissors were used to separate the animal's skin from the underlying muscle. Excess water was squeezed out of the CV sponges and two sponge/tubing assemblies were implanted in each animal—one on each side of the spine as shown in Fig. 2. The wounds were then closed with surgical staples.

Collagen gel preparation. Collagen gels were enclosed within 4-mm flat width hollow-fiber PVDF dialysis membranes with a 10^6-Da molecular weight cut-off so as to permit unhindered passage of all but the very largest soluble factors present in the wound environment yet prevent host inflammatory and tissue cells from invading or transplanted fibroblasts from leaving the gel. The flat membranes were expanded to a cylindrical geometry by flushing them with water. Membranes were rinsed in double-distilled water to remove traces of sodium azide from the storage solution and then wetted in 70% ethanol for approximately 45 min. Following ethanol wetting, care was take to prevent the membranes from drying. The membranes were transferred to double-distilled water, rinsed thoroughly, and then soaked for 30 min. Membranes were cut into approximately 2-cm lengths, transferred to a fresh double-distilled water bath, autoclaved, and kept in sterile water at 4°C until ready for use.

A 0.5% agarose solution was prepared by dissolving low-melting agarose in 25 mM Hepes-buffered saline; the solution was then autoclaved. Specially designed heating blocks containing 30 1.1-cm-diameter by 2.5-cm-deep holes were autoclaved, and 2 ml of sterile agarose was pipetted into each hole. The agarose-filled heating block was then transferred to a 4°C environment for at least an hour to induce agarose gelation. About 2 h before the experiment, the heating block was placed in an incubator to elevate the agarose temperature to 37°C. Just prior to the start of the experiment, the heating block was transferred to a dry bath set at 37°C.

Collagen solution at a concentration of 2.0 mg/ml was prepared from Vitrogen 100 type I collagen. Twenty microliters of 1 M Hepes buffer, 132 μl of 0.1 NaOH, 100 μl of 10× MEM, 60 μl of M199, 1 μl of pen–strep, and 10 μl of 30 mg/ml L-glutamine were combined with 677 μl of Vitrogen to yield 1 ml of approximately 2.0 mg/ml collagen solution at a pH of 7.4. RDFs were dispersed in the collagen solution at a concentration of 30,000 cells/ml.

A 2-cm section of sterile PVDF membrane was removed from the water bath using tweezers and shaken to remove water from the interior of the tube. The section of tubing was held horizontally, and 40 μl of the cell–collagen solution was pipetted inside the tube using a positive displacement pipet. Capillary action prevented the solution from running out of the tube. The end of a flat-bladed surgical clamp was heated to approximately 300°C and applied to both ends of the PVDF tubing to seal it. There was no obvious decrease in cell viability in the gel near the ends of the membrane due to the heat sealing process. We attribute this to the brevity of the sealing procedure (~2 s) and the poor thermal conductivity of PVDF. The sealed tube containing the solution was then placed upright in one of the 37°C agarose-containing holes of the heating block; the agarose prevented the membrane from drying out while keeping the gel upright so as to minimize the entrapment of air bubbles in the middle of the gel. The tube was left in the heating block for about 20 min to allow for collagen gelation before being placed in an incubator in a bath of 37°C saline solution. Tubes were kept in the saline solution until ready for implantation approximately an hour later.

Collagen gel insertion. Collagen gels were inserted into the sponge at an incision site distal to that of the CV sponge, thereby minimizing reinjury at the original wound site (Fig. 3). Following anesthetization of the rat, two small incisions were made near the ends of the Nalgene tubing. The thermoplastic adhesive was removed from the ends of the Nalgene tubes. The PVDF membrane enclosing the collagen gel was then attached to the Teflon thread inside the sponge/tubing assembly with a ligating clip (Ethicon, Sommerville, NJ), and the thread was pulled out the other side of the tubing until the gel was centered in the sponge. Excess Teflon thread was removed, the ends of the Nalgene tubing were resealed with thermoplastic adhesive, and the small incisions were closed with surgical staples.

Collagen gel removal and measurement. Gels were removed at either 2 or 4 days following their implantation in the CV sponge. The animal was sacrificed by CO_2 asphyxiation and an incision was made on its dorsal side. The sponge assembly was removed and the PVDF-enclosed gel was taken from the sponge and placed in 20 mM Hepes-buffered saline. Microscissors were used to cut open the PVDF membrane, and the gel was carefully removed from the membrane and maintained in saline.

An Olympus IX-70 inverted light microscope (Melville, NY) with automated stage and Photometrics cooled CCD camera (Tucson, AZ) was used to obtain a transmitted light mosaic image of the gels such as the ones shown in Fig. 4. Images of several gels were also taken immediately following gel formation in order to establish the initial size. Inovision ISee image analysis software (Raleigh, NC) was used to measure the gel diameter by averaging gel diameter measurements taken at three points along the length of the gel. The percentage compaction was then estimated by dividing the average compacted gel diameter by the average initial diameter. Statistical comparisons of compaction data was performed with ANOVA. Significance levels were set at $P < 0.05$.

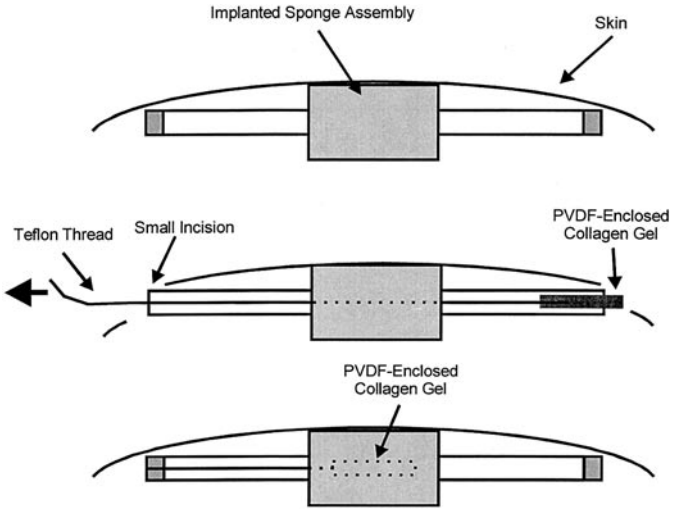

FIG. 3. Schematic of the collagen gel implantation method. Small incisions are made near the ends of the Nalgene tubes, and the ends are exposed. The thermoplastic adhesive is then removed. The PVDF membrane-enclosed collagen gel is then attached to a Teflon thread with a ligating clip, and the thread is pulled through the sponge assembly until the collagen gel is centered in the CV sponge. The ends of the Nalgene tubing are then resealed with thermoplastic adhesive, and the small incisions are closed with surgical staples.

Cell counts. Cells were counted using an adaptation of a previously developed technique [27]. Briefly, each gel was placed in 50 μl of 0.5 mg/ml collagenase and incubated at 37°C for 1 h. The cells were fixed by adding 65 μl of 4% paraformaldehyde, and 2 μl of propidium iodide was added to stain the cell nuclei. The cells were spun down in a well of a 96-well tissue culture plate, and an image of the well was taken under fluorescence illumination. Image analysis software was used to count the visible nuclei in the image. Statistical comparisons of cell counts were performed with ANOVA. Significance levels were set at $P < 0.05$.

Traction estimation. Our lab has previously developed a theory for cell–matrix mechanical interactions such as occur in the fibroblast-seeded collagen gel employed in this assay [28], and we have subsequently extended this theory to account for matrix fiber alignment that can occur during compaction [29]. However, because the gels employed in this assay are free-floating within the PVDF membrane (i.e., unconstrained), their compaction is uniform and no alignment should develop [29]. It is, therefore, sufficient to use the isotropic version of the theory for the data presented herein (see also Barocas *et al.* [30]). The details of the biphasic theory are presented in the Appendix. Briefly, five conservation equations (for cells and for mass and momentum of the fiber network and interstitial solution phases) are combined with two constitutive equations (network viscoelasticity and cell spreading) to relate the macroscopic compaction of the gel to the cell concentration and the average per-cell traction represented by the cell traction parameter, τ_0. Material properties for collagen gel have already been obtained by our lab as have estimates of cell spreading (i.e., time dependence of τ_0) and the cell migration coefficient [8, 31]. A summary of the parameter values used is presented in Table 1.

Using initial cell number and cell count data from the harvested gels, we can estimate a first-order rate constant for cell proliferation for each experimental condition by fitting the cell proliferation data to the integrated form of the equation

$$\frac{dn}{dt} = k_0 n,$$

where n is the cell number, t is time, and k_0 is the cell proliferation rate constant. Given the initial cell concentration, we can then use the biphasic theory to estimate τ_0 from the gel compaction data while accounting for the different cell proliferation rates under our various experimental conditions. The system of equations was solved using an FEM model combined with the COOPT optimization routine as described elsewhere [32, 33].

Actin staining. Recovered gels were fixed for 60 min in 4% paraformaldehyde and then rinsed with PBS containing 0.3% Triton (PBST). Gels were then blocked for 60 min with 10% normal goat serum. Anti-α-smooth muscle actin monoclonal antibody was diluted 1:100, and the gels were incubated in this antibody solution overnight. The next day, gels were rinsed with PBST before being incubated for 60 min with goat anti-mouse Alexa 488 secondary antibody at a 1:100 dilution. TRITC-conjugated phalloidin was also added at a 1:100 dilution to stain for F-actin [34]. Gels were then rinsed with PBST and mounted on a slide with DAPI mounting medium (Vector Laboratories, Burlingame, CA).

Mechanical testing. An Instron (Canton, MA) planar biaxial tester configured in uniaxial mode with resolution on the order of 0.1 mN was used to determine the ultimate tensile strength of the recovered gels as described elsewhere [27]. Briefly, the gels were gripped with spring-loaded tissue grips and stretched at a constant strain rate until failure. Reported stress values were based upon estimated gel cross-sectional area prior to stretching.

RESULTS

Two postwounding time frames were investigated: the 1- to 5-day period and the 7- to 11-day period. In both cases, the time of wounding (CV sponge implantation) was designated day 0. For the 1- to 5-day period, PVDF tubes containing gels were inserted into the implanted sponge on the 1st day after wounding and harvested on the 3rd and 5th days. For the 7- to 11-day time frame, gels were inserted on the 7th day and harvested on the 9th and 11th days. Paired gels were maintained in culture in complete medium for comparison.

Gel compaction. Average gel diameter over time is presented in Fig. 5 for the two time frames. Three gels were used to estimate average gel diameter at each time point. In the day 1–5 wounds, the implanted gels compacted more rapidly by day 3 and by day 5 than gels cultured over the same time (ANOVA, $P < 0.02$). However, the gels implanted in day 7–11 wounds compacted at about the same rate as gels cultured over the same time. The amount of compaction in day 1–5 wounds was also significantly greater than compaction in day 7–11 wounds (ANOVA, $P < 0.02$). Compaction did not statistically differ between *in vitro* controls for day 1–5 and day 7–11 experiments.

Cell number. Cell counts for the various gels are presented in Fig. 6. Cells from three gels were counted to estimate average cell number at each time point. In day 1–5 wounds, cell number increased approximately 30% in the implanted gels while there was essentially no change in cell number in gels cultured during the same time. This increase was not statistically significant (ANOVA, $P = 0.11$). In day 7–11 wounds, there

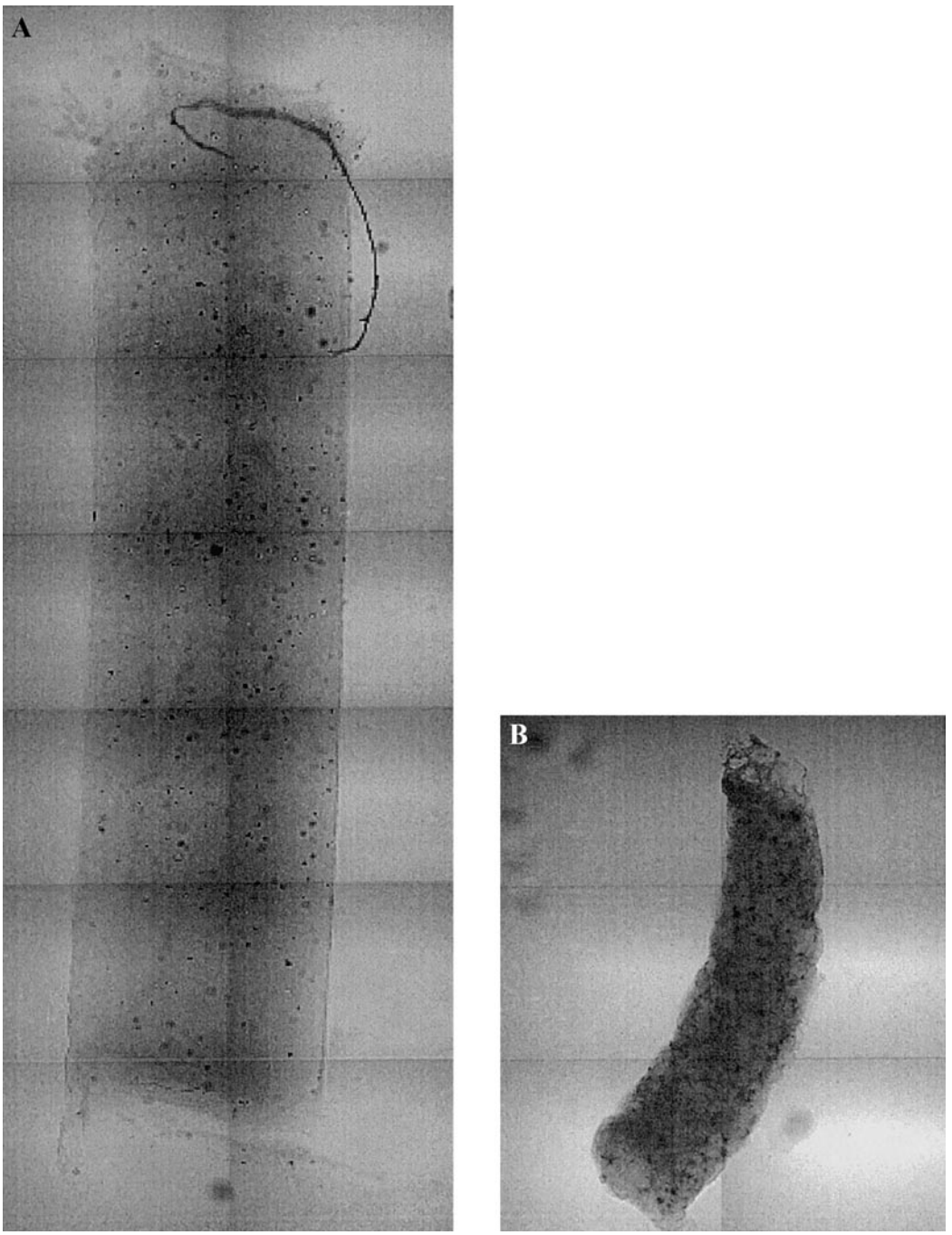

FIG. 4. Image of a typical collagen gel following removal from the PVDF membrane (A) shortly after gel formation and (B) after 4-day implantation. The small dark dots throughout the gel are RDFs.

was a significant increase ($P < 0.001$) in cell number of about 160% over the 4-day implantation period while no significant change in cell number occurred in gels cultured during the same time. The increase in cell number in day 7–11 wounds was also significantly different from the increase in day 1–5 wounds (ANOVA, $P < 0.01$). The first-order rate constants for cell proliferation are presented in Table 2. Proliferation did not differ statistically between the controls for day 1–5 and for day 7–11 experiments.

Traction estimation. The resulting best-fit values for τ_0 are presented in Table 3 for the various experimental conditions. RDFs implanted in day 1–5 wounds had a 30% higher traction than those from gels simultaneously maintained in culture. However, RDFs implanted in day 7–11 wounds exhibited 27% lower trac-

TABLE 1

Biphasic Theory Model Parameters

Parameter	Parameter value	Reference
Collagen network		
Shear modulus, G (dyne/cm^2)	11,850	[31]
Shear viscosity, η (dyne · s/cm^2)	1.24×10^8	[31]
Drag coefficient, ϕ_0 (dyne · s/cm^4)	6.4×10^6	[31]
Poisson's ratio, ν (dimensionless)	0.2	[57]
Fibroblasts		
Migration coefficient, D_0 (cm^2/s)	1.7×10^{-10}	[29]
Spreading steepness, k_{sp} (dimensionless)	1.6	[8]
Spreading half time, $t_{1/2}$ (h)	4	[8]

tion then those maintained in culture over the same period. Only one estimation of τ_0 could be determined for each condition because all gel compaction values were reduced to one compaction curve for each condition. Therefore, no statistical comparison of τ_0 could be performed.

Cell morphology. Images of typical cells from both the control and the implanted gels are presented in Fig. 7. While cell morphology in the gels was variable, these cells are representative of the predominant morphology present under each set of conditions. The cells from the implanted gels exhibited an elongated, polar morphology in both the day 1–5 and the day 7–11 wounds while the cells from cultured gels were typically stellate.

Actin staining. Typical results for α-smooth muscle actin and F-actin staining are presented in Fig. 8. In gels maintained in culture, more than half of the cells expressed α-smooth muscle actin. In the implanted gels from both the 1- to 5- and the 7- to 11-day periods there were almost no cells expressing α-smooth muscle actin.

Mechanical testing. Ultimate tensile strength measurements for implanted and control gels are presented in Table 4. There was no difference in ultimate tensile strength between gels maintained in culture and those implanted in the rat for 4 days.

DISCUSSION

Methods for a novel implantable collagen gel assay for fibroblast proliferation and traction have been presented. Fibroblast-populated collagen gels contained within a PVDF semipermeable membrane were placed within an implanted CV sponge at selected times following the initial wounding. Gels were subsequently removed and both the gel diameter and the cell number determined. Gel compaction of and cell proliferation in implanted gels populated by dermal fibroblasts were different from those of gels maintained in culture. Compaction and proliferation results were also different depending on the time frame during which the gels were placed in the wound site.

The rate of gel compaction is a function of both the cell number and the per-cell traction if the mechanical properties of the gel are constant. In our various *in vitro* assays for cell traction, cell proliferation rates have not varied significantly under the experimental conditions. As a result, for a given cell concentration, the differences in gel compaction can be tied directly to differences in cell traction [8, 11]. In this study, how-

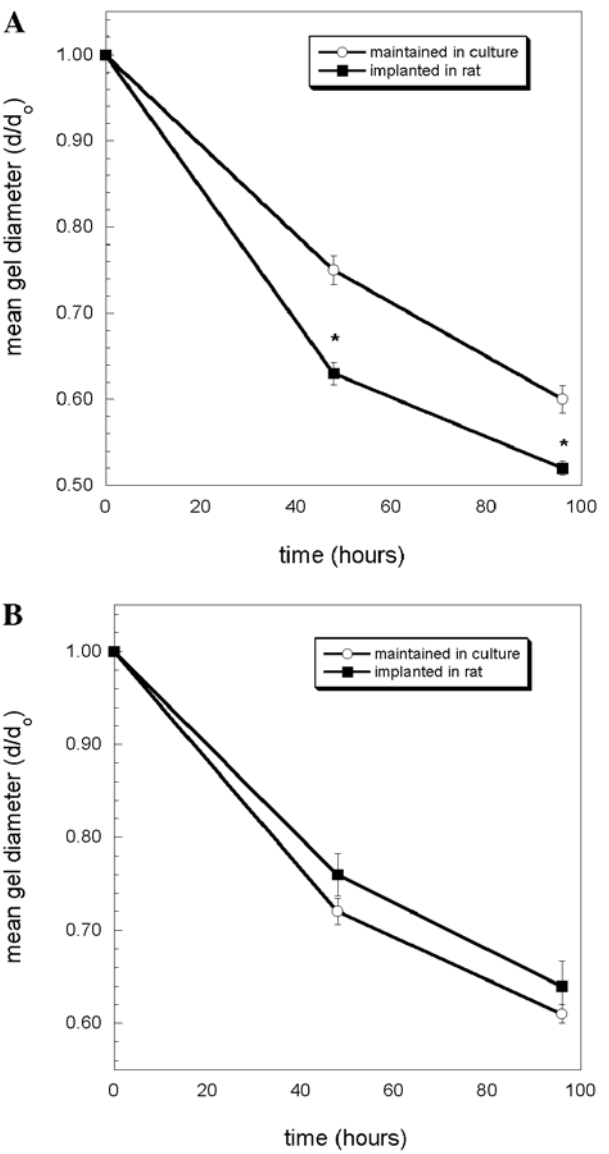

FIG. 5. Compaction data for gels maintained in culture and gels implanted in rats from (A) days 1–5 and (B) days 7–11. In day 1–5 wounds, the gels compact more rapidly than those maintained in culture (*ANOVA, $P < 0.02$). In day 7–11 wounds, the compaction of implanted gels is only slightly less than that of those maintained in culture and not significantly different. The compaction in day 1–5 wounds is also significantly greater than the compaction in day 7–11 wounds (ANOVA, $P < 0.02$).

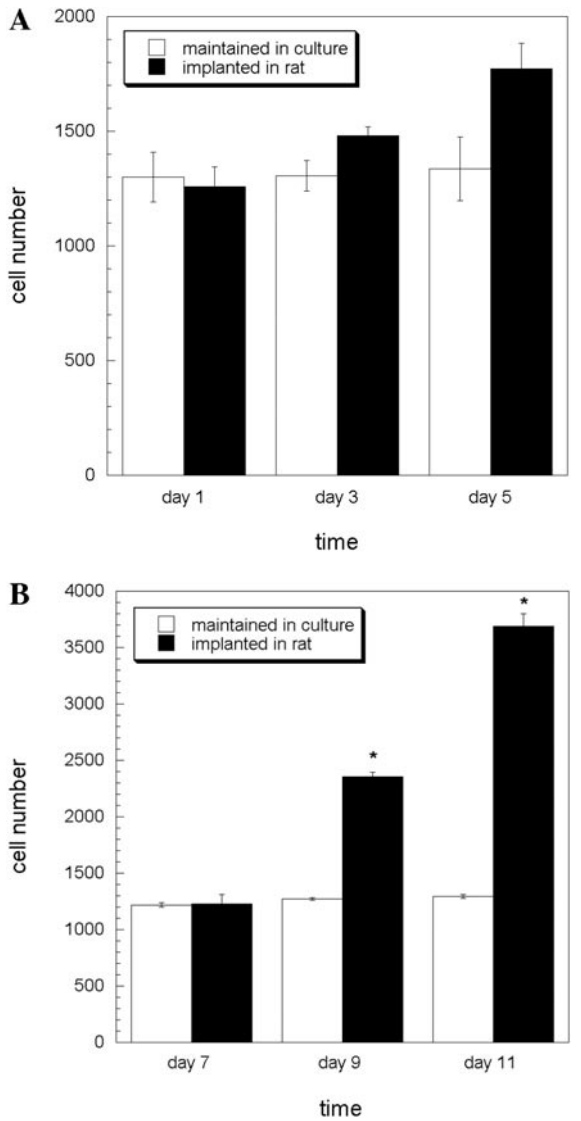

FIG. 6. Cell counts from control gels maintained in culture and gels implanted in rats from (A) days 1–5 and (B) days 7–11. Cell numbers for RDFs in gels maintained in culture do not change much over the course of the experiment. In contrast, cell numbers in the implanted gels increase over the implantation period. The increase is statistically significant in day 7–11 wounds (*ANOVA, $P < 0.001$). Cells were counted immediately after gels were harvested from the wound. The cell number in day 7–11 wounds is also significantly greater than cell number in day 1–5 wounds (ANOVA, $P < 0.01$).

ever, we observed large differences in the cell proliferation rates depending upon the time frame postwounding during which the gel was implanted. This is not unexpected since the wound site contains a plethora of growth factors with varying mitogenic potential whose concentrations change over the course of the wound healing response [12, 35–38]. To obtain an accurate estimate of cell traction in our implantable assay, we accounted for a variable cell proliferation rate (i.e., different values of k_0 for the two wound periods studied).

TABLE 2

First-Order Cell Proliferation Rate Constants

Conditions	k_0 (s^{-1}) $\times 10^7$
Days 1 to 5	
Maintained in culture	0.76 ± 0.30
Implanted in rat	9.92 ± 0.27
Days 7 to 11	
Maintained in culture	1.76 ± 0.38
Implanted in rat	31.83 ± 3.41

The proliferation rate constants for cells in the cultured gels were comparatively low (Table 2). This is consistent with previous observations that fibroblast proliferation is depressed in collagen gels [39]. The wound environment is replete with growth factors such as PDGF that are highly mitogenic for fibroblasts [1], so it is not surprising that we observed increased proliferation in the implanted gels. The significantly higher proliferation rate in day 7–11 wounds versus day 1–5 wounds (ANOVA, $P < 0.05$) is attributed to the time-varying composition of the wound environment. Various growth factors have been shown to have temporally varying concentrations in the wound [12, 37, 38]. It is likely that the concentrations and combinations of growth factors present during the 7- to 11-day period in our assay are simply more mitogenic for fibroblasts than the concentrations and combinations present during the 1- to 5-day period. Such temporal variation in growth factor concentration helps drive the wound healing response through its various phases.

In the day 1–5 wounds, the implanted gels compacted more rapidly than those maintained in culture (Fig. 5A). If not for the difference in cell proliferation between the two experimental conditions (Fig. 6A), this difference in compaction rate for gels that have similar mechanical properties (Table 4) would lead us to conclude that the fibroblasts exposed to the day 1–5 wound environment exhibited higher traction than their counterparts maintained in culture. However, without the use of the biphasic theory for cell–matrix mechanical interactions that allows us to account for the differ-

TABLE 3

Cell Traction Parameter Values from Biphasic Theory Data Fits

Conditions	τ_0 (dyn cm/cell) $\times 10^2$
Days 1 to 5	
Maintained in culture	1.57 ± 0.07
Implanted in rat	2.05 ± 0.10
Days 7 to 11	
Maintained in culture	1.62 ± 0.06
Implanted in rat	1.18 ± 0.10

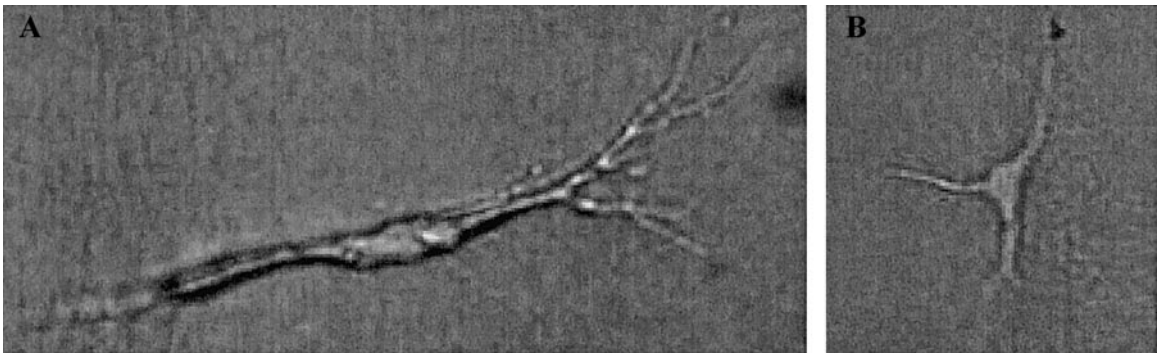

FIG. 7. Images of representative cells from gels (A) implanted in a rat and (B) maintained in culture. Images were taken at the same magnification. Cells from implanted gels exhibit an elongated, polar morphology that is often correlated with rapid cell migration in our *in vitro* assays (e.g., when stimulated with PDGF BB). Cells from gels maintained in culture display a stellate morphology that is not typically associated with migration in our *in vitro* assays.

ences in cell proliferation, we would be unable to draw any conclusion about the traction of implanted cells relative to those maintained in culture. Table 3 indicates that despite the higher cell proliferation rate, RDFs in collagen gels exposed to the day 1–5 wound environment did, indeed, exert a greater traction than RDFs in cultured gels.

We observed that the RDFs in collagen gels exposed to the later wound environment (days 7–11) behaved different from those exposed to the early wound environment. The compaction curve of gels from day 7–11 wounds was very similar to that of those maintained in culture (Fig. 5B). However, the implanted RDFs had a much higher proliferation rate (Fig. 6B). Given the similar gel compaction rates and gel mechanical properties, and the large difference in proliferation, RDFs implanted in the wound site must have a lower traction compared to RDFs in cultured gels, and this is borne out by the results of fitting the biphasic theory to the data as shown in Table 3. Note that the cultured gels paired to the day 1–5 and day 7–11 experiments had similar traction values (Table 3). As these cells were not implanted but simply maintained in culture, they were exposed to identical conditions and would be expected to exhibit similar traction.

Fibroblasts constitutively express F-actin as part of their cytoskeleton [40], and this is clearly seen in the staining shown in Fig. 8. Under certain conditions, fibroblasts will express some of the phenotypic markers of smooth muscle cells, α-smooth muscle actin in particular [41]. These cells are known as myofibroblasts and are believed to play a role in wound contraction and tissue restructuring [42]. Myofibroblasts are also routinely found in populations of cultured fibroblasts [43], and fibroblast α-smooth muscle actin expression increases in response to transforming growth factor β stimulation and mechanical stress in collagen gels [44]. Further, our *in vitro* studies reveal that these high-traction fibroblasts found in stressed collagen gels exhibit low migration [11]. As shown in Fig. 8A, cells in our cultured collagen gels exhibited both typical fibroblast and myofibroblast phenotypes. However, hardly any myofibroblasts were present in our implanted gels. It appears that the soluble wound environment of both the 1- to 5- and the 7- to 11-day periods down-regulated α-smooth muscle actin expression and inhibited the myofibroblastic phenotype.

Traction is necessary for cell migration and restructuring of surrounding tissue fibers although the amount of traction required for both may differ [45]. Given that fibroblast migration and tissue restructuring are both crucial elements of the wound healing response, it is reasonable to expect that RDF traction would vary depending on the stage of wound healing. We have previously reported that PDGF BB increases the traction of RDFs in free-floating (stress-free) collagen gels *in vitro* [11]. It is also well known that the various PDGF isoforms are abundant in the early wound environment [46], though our own analysis of rat wound fluid has indicated that the PDGF BB concentration in the early wound is about an order of magnitude lower than that needed to produce an optimal response in our *in vitro* assays (unpublished data). Since our implantable collagen gel was free-floating (i.e., it does not adhere to the PVDF membrane), the increase in RDF traction that we report herein for RDF implanted in day 1–5 wounds is consistent with our *in vitro* findings, especially if PDGF is one of the primary modulators of RDF traction in the early wound. Further, our *in vitro* studies revealed that the increase in RDF traction upon PDGF BB stimulation was correlated with an increase in fibroblast random migration [11]. While we are unable to directly measure migration in the implanted collagen gel, we can observe the cell morphology upon gel harvest. RDFs in implanted gels from both time periods tended to have an elongated, polar morphology in contrast to the stellate morphology observed in gels maintained in culture (Fig. 7). In our *in vitro* studies, PDGF BB-stimulated migrating cells tend to have an elongated, bipolar morphology

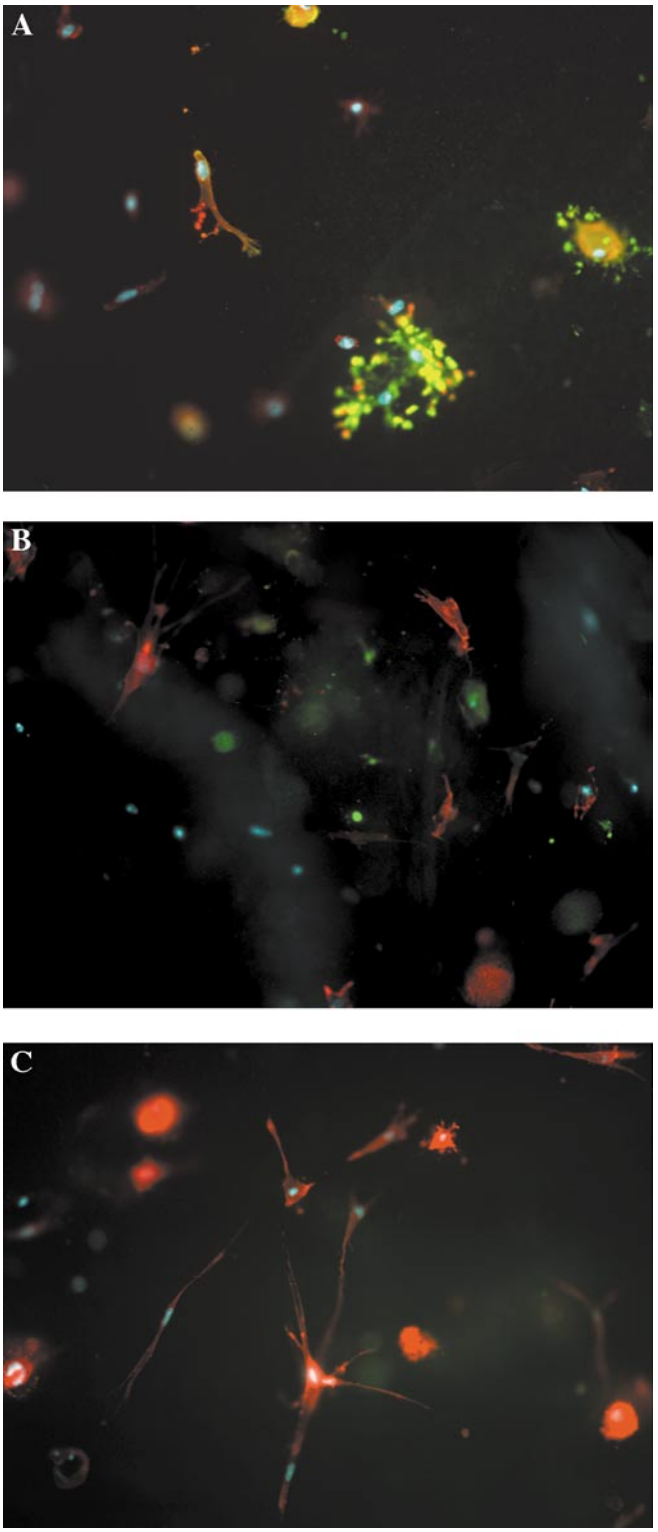

FIG. 8. Staining for F-actin and α-smooth muscle actin in gels (A) maintained in culture, (B) implanted from day 1 to 5, and (C) implanted from day 7 to 11. Cell nuclei are stained blue. Red indicates positive F-actin staining while green indicates positive α-smooth muscle actin. Cells expressing both F-actin and α-smooth muscle actin appear orange. More than half the cells in the cultured gel expressed α-smooth muscle actin while almost none implanted in the day 1–5 or 7–11 wounds did.

TABLE 4

Ultimate Tensile Strength Measurements for Implanted and Control Gels

Conditions	Ultimate tensile strength $\times 10^{-4}$ (dyn/cm^2)
Maintained in culture	1.04 ± 0.12
Implanted from day 1 to 5	1.07 ± 0.17
Implanted from day 7 to 11	1.06 ± 0.08

very similar to that observed in the implanted gels while cells with a stellate morphology tend not to migrate [8]. As noted above, the lack of α-smooth muscle actin expression in the implanted gels is also consistent with a migratory cell phenotype. Taken together, these observations suggest that cells in the implanted gels are stimulated to migrate by the growth factors present in the day 1–5 and 7–11 wound environments.

It is more difficult to interpret the observed decrease in traction during the 7- to 11-day period. During wound healing, fibroblasts sequentially migrate into the wound site, proliferate, synthesize ECM, remodel the tissue through matrix degradation and tractional restructuring (sometimes leading to wound contraction), and eventually recede from the wound site [1]. The duration of each of these steps in the sequence depends upon the nature of the wound, the species of the animal, and the unique biology of the individual. Moreover, the CV sponge itself can affect the time course of wound healing. Sponge size, composition, and porosity have been shown to affect the rate of granulation tissue formation in the sponge model [47] and, in our experience, the biological properties of wound fluid harvested from such sponges (unpublished observations). So, while it is reasonable to conclude that during days 1–5 of the wound healing response fibroblasts were in the process of migrating into the wound site and proliferating, it is less obvious what their predominant activity was during the day 7–11 period. Specifically, it is not clear in our assay whether fibroblasts have yet entered the matrix formation and remodeling phase of wound healing. Therefore, it is difficult to correlate the observed RDF traction with some specific wound healing behavior. A histological analysis of the wound and the determination of the levels of key growth factors in wound fluid taken from that time period might help put the observed decrease in traction in context. However, the high rate of proliferation seen during the 7- to 11-day period (Table 2) suggests that the fibroblasts implanted in the wound were still primarily engaged in the proliferative phase of the wound healing response.

It should be noted that our *in vitro* studies indicate that the mechanical stress state of the gel modulates RDF response to PDGF BB stimulation [11]. Others have observed morphological and metabolic differences

in cells depending on the stress state of the matrix [44, 48–50]. As a mechanically constrained tissue that has undergone platelet retraction and perhaps some amount of wound contraction, the provisional matrix of the early wound is arguably more like a stressed collagen gel than the unstressed one used in our implantable assay. Given that the stress state of the ECM is known to affect cellular behavior, differences between the stress state of our implantable gel and the wound tissue itself must be considered when interpreting the results.

A pure collagen gel is quite different from the provisional wound matrix of fibrin, collagen, fibronectin, and other matrix molecules [1]. It is well known that the ECM mediates cell phenotype and modulates responses to growth factors [1, 51, 52]. Normally, signals from early wound fluid would be combined with signals from the predominantly fibrin provisional wound matrix [1]. Therefore, the cells in our assay, because they are seeded in collagen, may be receiving abnormal cues for a wound environment. So, both the stress state and the composition of the gel used in these studies may diminish the physiological relevance of our results.

While the implantable free-floating collagen gel is clearly not a direct analog of wound tissue, it does provide a defined, reproducible, three-dimensional biological reference matrix for studying cellular behavior. The assay allows us to study the effect of the soluble wound environment on cells in the reference matrix, and more importantly, it also allows us to study how the effect of the soluble wound environment changes over the course of the wound healing response. Further, we are exploring ways to create a version of the assay that includes a mechanical constraint on compaction that would allow us to investigate the role of mechanical stress on fibroblast behavior *in vivo*. Additionally, we could use fibrin gel in place of collagen, but attempts to prevent fibrin from adhering strongly to the PVDF membrane, thereby preventing gel compaction, have not yet been successful. Similarly, fibrinolysis might alter the mechanical properties of the gel and complicate the use of our theory for cell–matrix mechanical interactions to infer cell traction from gel compaction.

Because of the differences in cell proliferation rates observed under our various experimental conditions, we have used the biphasic theory for cell–matrix mechanical interactions to estimate cell traction. In doing so, we have made implicit assumptions about the mechanical properties of the collagen gel. Shear [30] and compression [31] experiments have shown the collagen network to exhibit viscoelastic fluid behavior. For simplicity, the network is modeled as a single relaxation time compressible Maxwell fluid [29]. This assumption has been shown to yield fairly accurate results for cell compaction of collagen gels up to about a 15% strain [53]. It is clear from Fig. 5 that the implantable gels experience strains of nearly 50% at the later time points. At these higher strains, the model fit becomes poorer and the resulting estimate of τ_0 is less accurate. However, we are still able to undertake a comparative analysis of τ_0 and can conclude that the traction exerted by cells implanted in day 1–5 wounds is greater than that of those maintained in culture and those implanted in day 7–11 wounds.

Our ability to perform a comparative analysis of cell traction rests upon the assumption that the mechanical properties of the collagen network do not differ significantly from one gel to another. We have established *in vitro* that the gel properties are relatively constant if the gels are formed under the same conditions [31]. However, *in vivo* we introduce additional variables. Specifically, we must consider the possible effects of proteinases present during wound healing that may degrade the collagen and alter the network properties. Our implantable gel is composed of type I collagen, and a group of matrix metalloproteinases that degrade collagen, the collagenases, is found in the wound [54].

To attempt to assess possible degradation, we mechanically tested several gels in uniaxial extension. We compared the ultimate tensile strength of implanted gels to that of those maintained in culture. As shown in Table 4 there was no significant difference. Due to the small size and relatively weak nature of our gels, accurate measurement of the ultimate tensile strength was difficult. The load at failure was only about three to four times the force resolution limit for the mechanical test system, so small changes in the gel mechanical properties due to collagen degradation were not detectable. Nevertheless, the ultimate tensile strength measurements provided no evidence of large differences in terms of mechanical properties between gels maintained in culture and those implanted in wounds that might invalidate the assumptions of the biphasic theory. Degradation of the matrix and the resulting change in mechanical properties may be a more significant concern if the gels are exposed to the wound environment for longer periods of time or implanted at later time points such as during the tissue remodeling phase when collagenase activity may be higher.

This assay combines the more quantitative nature of *in vitro* assays with the greater physiological relevance of *in vivo* wound healing models. Cells are exposed to the soluble wound environment but otherwise isolated from the host animal. As the cells are sequestered within the PVDF dialysis membrane, they can be recovered from the wound at prescribed time points. We have demonstrated herein the ability to quantify fibroblast proliferation and traction upon exposure to the soluble wound environment using the assay. There are, however, a number of other ways in which the unique

features of this assay could be employed. Though we have not done so, wound fluid could also be harvested from the CV sponge and its composition analyzed and correlated with the time varying cell behavior. Syngeneic cells other than dermal fibroblasts could be implanted. Endothelial cells have been shown to form tubes in three-dimensional collagen gels *in vitro* [55]; the effect of the soluble wound environment on this behavior could readily be studied using our assay. Genetically modified cells that are unresponsive to certain growth factors could be implanted and the assay used to assess the role of these growth factors in modulating cell behavior in wound healing. Using the dominant negative receptor technique [56], we are currently developing a fibroblast that lacks signaling capability through the PDGF β receptor so that we can probe the role of PDGF BB in regulating fibroblast traction and proliferation in the wound. Herein, we have used immunocytochemical techniques to study the expression of α-smooth muscle actin by cells in implanted gels. Similar methods could be used to probe for the expression of other proteins. Alternatively, mRNA levels could be measured to assess gene expression.

APPENDIX

The biphasic theory for cell–matrix mechanical interactions has been described in detail elsewhere [28, 29]. We provide a brief overview here of the isotropic version of the theory for the assay presented.

The model consists of five conservation equations and two constitutive equations. The mass conservation equations for the network and solution phases in terms of volume fractions θ_n and θ_s are

$$\frac{D\theta_n}{Dt} + \theta_n(\nabla \cdot \mathbf{v}_n) = 0, \tag{1}$$

$$\frac{D\theta_s}{Dt} + \theta_s(\nabla \cdot \mathbf{v}_s) = 0, \tag{2}$$

where $\mathbf{v}_n$ and $\mathbf{v}_s$ are the velocities of the phases and D/Dt denotes the substantial derivative moving with each phase. The momentum conservation equations for the solution and network are

$$\nabla \cdot [\theta_s(P\mathbf{I})] + \phi(\mathbf{v}_s - \mathbf{v}_n) = 0, \tag{3}$$

$$\nabla \cdot [\theta_n(\sigma + c\tau_0\mathbf{I} - P\mathbf{I})] + \phi(\mathbf{v}_s - \mathbf{v}_n) = 0, \tag{4}$$

where P is the hydrostatic pressure, ϕ_0 is an interstitial drag coefficient between the network and the solution phases, σ is the network viscoelastic stress tensor, and τ_0 is the cell traction parameter.

The cell conservation equation accounting for cell proliferation, convection, and migration is

$$\frac{Dc}{Dt} + c(\nabla \cdot \mathbf{v}_n) = D_0\nabla^2 c + k_0 c, \tag{5}$$

where c is the cell concentration, D_0 is the cell migration coefficient, and k_0 is the first-order rate constant for cell proliferation. Since the cells are considered a species in the network phase (in which they are convected and migrate and must attach for proliferation), the cell concentration is defined per unit volume of network phase and the substantial derivative is with respect to $\mathbf{v}_n$.

The network was modeled using the single relaxation time compressible Maxwell fluid equation, which has been shown to be of sufficient accuracy for compacting gels up to about 15% strain [30, 53],

$$\frac{1}{2G}\,\dot{\sigma} + \frac{1}{2\eta}\,\sigma = \tfrac{1}{2}\,[\nabla\mathbf{v}_n + (\nabla\mathbf{v}_n)^T] + \frac{\upsilon}{1-2\upsilon}\,(\nabla \cdot \mathbf{v}_n)\mathbf{I}, \tag{6}$$

where G is the shear modulus, η is the shear viscosity, and υ is Poisson's ratio. The dot denotes the upper-convected derivative.

In order to account for cell spreading and development of motility from an initial nonmotile state when the gel is formed, the cell migration and traction stress coefficients were modified accordingly with a sigmoidal dependence on time [28, 30],

$$D_0(t) = D_0\,\frac{t^{(k_{sp})}}{t^{(k_{sp})} + (t_{1/2})^{(k_{sp})}}, \tag{7}$$

$$\tau_0(t) = \tau_0\,\frac{t^{(k_{sp})}}{t^{(k_{sp})} + (t_{1/2})^{(k_{sp})}}, \tag{8}$$

where k_{sp} determines the steepness of the spreading vs time response and $t_{1/2}$ is the half time for cell spreading.

For the case of the cylindrical collagen gel used to model our implantable assay, the boundary conditions for the symmetry plane and axis of the cylinder are

$$v_n = (\sigma + \tau_0 c\mathbf{I})_{nt} = \frac{\partial c}{\partial n} = \frac{\partial P}{\partial n} = 0, \tag{9}$$

where v is a component of the network velocity and n and t refer to the normal and tangent directions. The boundary conditions for the surfaces are

$$P = (\sigma + \tau_0 c\mathbf{I})_{nn} = (\sigma + \tau_0 c\mathbf{I})_{nt} = \frac{\partial c}{\partial n} = 0. \tag{10}$$

τ_0 is estimated by fitting the gel compaction data (network displacement data) to the model equations using a finite element method to discretize the spatial deriv-

atives in combination with the optimal control algorithm for differential algebraic equation systems, COOPT [32, 33].

ACKNOWLEDGMENTS

The authors thank Cynthia Coulter and Luca Gunther for assisting with the animal surgeries, Michael Neidert for assistance with mechanical testing, and Malcolm Morrison at Spectrum Labs for providing the PVDF dialysis tubing. This work was supported by NIH P01-GMS0150-03S1 (R.T.T.) and a graduate fellowship from the Whitaker Foundation (P.A.J.E.).

REFERENCES

1. Clark, R. A. F. Wound repair: Overview and general considerations. In R. A. F. Clark (Ed.), *The Molecular and Cellular Biology of Wound Repair*. New York: Plenum, 1996. Pp. 3–50.
2. Van Winkle, W., Jr. Wound contraction. *Surg. Gynecol. Obstet.* **125:** 131, 1967.
3. Ramirez, A. T., Soroff, H. S., Schwartz, M. S., Mooty, J., Pearson, E., and Raben, M. S. Experimental wound healing in man. *Surg. Gynecol. Obstet.* **128:** 283, 1969.
4. Grinnell, F. Fibroblasts, myofibroblasts, and wound contraction. *J. Cell Biol.* **124:** 401, 1994.
5. Moghe, P. V., Nelson, R. D., and Tranquillo, R. T. Cytokine-stimulated chemotaxis of human neutrophils in a 3-D conjoined fibrin gel assay. *J. Immunol. Methods* **180:** 193, 1995.
6. Knapp, D. M., Helou, E. F., and Tranquillo, R. T. A fibrin and collagen gel assay for tissue cell chemotaxis: Assessment of fibroblast chemotaxis to GRGDSP. *Exp. Cell Res.* **247:** 543, 1999, doi: 10.1006/excr.1998.4364.
7. Guido, S., and Tranquillo, R. T. A methodology for the systematic and quantitative study of cell contact guidance in oriented collagen gels. *J. Cell Sci.* **105:** 317, 1993.
8. Knapp, D. M., Tower, T. T., Tranquillo, R. T., and Barocas, V. H. Estimation of cell traction and migration in an isometric cell traction assay. *AIChE J.* **45:** 2628, 1999.
9. Moon, A. G., and Tranquillo, R. T. Fibroblast-populated collagen microsphere assay of cell traction force. Part 1.Continuum model. *AIChE J.* **39:** 163, 1993.
10. Dickinson, R. B., and Tranquillo, R. T. Optimal estimation of cell movement indices from the statistical analysis of cell tracking data. *AIChE J.* **39:** 1995, 1993.
11. Shreiber, D. I., Enever, P. A. J., and Tranquillo, R. T. Effects of PDGF-BB on rat dermal fibroblast behavior in mechanically stressed and unstressed collagen and fibrin gels. *Exp. Cell Res.* **266:** 155, 2001, doi: 10.1006/excr.2001.5208.
12. Dvonch, V. M., Murphey, R. J., Matsuoka, J., and Grotendorst, G. R. Changes in growth factor levels in human wound fluid. *Surgery* **112:** 18, 1992.
13. Paul, R. G., Tarlton, J. F., Purslow, P. P., Sims, T. J., Watkins, P., Marshall, F., Ferguson, M. J., and Bailey, A. J. Biomechanical and biochemical study of a standardized wound healing model. *Int. J. Biochem. Cell Biol.* **29:** 211, 1997.
14. Mustoe, T. A., Pierce, G. F., Morishima, C., and Deuel, T. F. Growth factor-induced acceleration of tissue repair through direct and inductive activities in a rabbit dermal ulcer model. *J. Clin. Invest.* **87:** 694, 1991.
15. Kivisaari, J., and Niinikoski, J. Effects of hyperbaric oxygenation and prolonged hypoxia on the healing of open wounds. *Acta Chir. Scand.* **141:** 14, 1975.
16. Wiener, S. L., Wiener, R., Platt, N., Urivetzky, M., and Meilman, E. The need for modification of the polyvinyl sponge model of connective tissue growth. Histologic and biochemical studies in the rabbit. *Connect. Tissue Res.* **3,** 213, 1975.
17. Diegelmann, R. F., Lindblad, W. J., and Cohen, I. K. A subcutaneous implant for wound healing studies in humans. *J. Surg. Res.* **40:** 229, 1986.
18. Paulini, K., Korner, B., Beneke, G., and Endres, R. A quantitative study of the growth of connective tissue: Investigations on implanted polyester–polyurethane sponges. *Connect. Tissue Res.* **2:** 257, 1974.
19. Holm-Pedersen, P., and Zederfeldt, B. Granulation tissue formation in subcutaneously implanted cellulose sponges in young and old rats. *Scand. J. Plast. Reconstr. Surg.* **5:** 13, 1971.
20. Niinikoski, J., Heughan, C., and Hunt, T. K. Oxygen and carbon dioxide tensions in experimental wounds. *Surg. Gynecol. Obstet.* **133:** 1003, 1971.
21. Viljanto, J. Cellstic: A device for wound healing studies in man. Description of the method. *J. Surg. Res.* **20:** 115, 1976.
22. Jorgensen, L. N., Kallehave, F., Karlsmark, T., Vejlsgaard, G. L., and Gottrup, F. Evaluation of the wound healing potential in human beings from the subcutaneous insertion of expanded polytetrafluoroethylene tubes: A methodologic study. *Wound Repair Regener.* **2:** 20, 1994.
23. Alaish, S. M., Bettenger, D. A., Olutoye, O. O., Gould, L. J., Yager, D. R., Davis, A., Crossland, M. C., Diegelmann, R. F., and Cohen, K. Comparison of polyvinyl alcohol sponge and expanded polytetrafluoroethylene subcutaneus implants as models to evaluate wound healing potential in human beings. *Wound Repair Regener.* **3:** 292, 1995.
24. Schilling, J. A., Joel, W., and Shurley, H. M. Wound healing: A comparative study of the histochemical changes in granulation tissue contained in stainless steel wire mesh and polyvinyl sponge cylinders. *Surgery* **46:** 702, 1959.
25. Wicke, C., Halliday, B. J., Scheuenstuhl, H., Foree, E. F., and Hunt, T. K. Examination of expanded polytetrafluoroethylene wound healing models. *Wound Repair Regener.* **3:** 284, 1995.
26. Freshney, R. I. *Culture of Animal Cells: A Manual of Basic Technique*, 2nd ed., New York: A. R. Liss, 1987.
27. Girton, T. S., Oegema, T. R., Grassl, E. D., Isenberg, B. C., and Tranquillo, R. T. Mechanisms of stiffening and strengthening in media-equivalents fabricated using glycation. *J. Biomech. Eng.* **122:** 216, 2000.
28. Barocas, V. H., and Tranquillo, R. T. Biphasic theory and in vitro assays of cell–fibril mechanical interactions in tissue-equivalent gels. In V. C. Mow, F. Guilak, R. Tran-Son-Tay and R. M. Hochmuth (Eds.), *Cell Mechanics and Cellular Engineering*. New York: Springer-Verlag, 1994. Pp. 185–209.
29. Barocas, V. H., and Tranquillo, R. T. An anisotropic biphasic theory of tissue-equivalent mechanics: The interplay among cell traction, fibrillar network deformation, fibril alignment, and cell contact guidance. *J. Biomech. Eng.* **119:** 137, 1997.
30. Barocas, V. H., Moon, A. G., and Tranquillo, R. T. The fibroblast-populated collagen microsphere assay of cell traction force. Part 2. Measurement of the cell traction parameter. *J. Biomech. Eng.* **117:** 161, 1995.
31. Knapp, D. M., Barocas, V. H., Moon, A. G., Yoo, K., Petzold, L. R., and Tranquillo, R. T. Rheology of reconstituted type I collagen gel in confined compression. *J. Rheol.* **41:** 971, 1997.
32. Barocas, V. H., and Tranquillo, R. T. A finite element solution for the anisotropic biphasic theory of tissue-equivalent mechanics: The effect of contact guidance on isometric cell traction measurement. *J. Biomech. Eng.* **119:** 261, 1997.
33. Serban, R., and Petzold, L. R. COOPT—A software package for optimal control of large-scale differential algebraic equation systems. *Math. Comput. Simul.* **56:** 187, 2001.
34. Hedberg, K. M., and Bell, P. B., Jr. The effect of neomycin on

PDGF-induced mitogenic response and actin organization in cultured human fibroblasts. *Exp. Cell Res.* **219:** 266, 1995.

35. Ono, I., Gunji, H., Zhang, J.-Z., Maruyama, K., and Kaneko, F. Studies on cytokines related to wound healing in donor site wound fluid. *J. Dermatol. Sci.* **10:** 241, 1995.
36. Ono, I., Gunji, H., Zhang, J.-Z., Maruyama, K., and Kaneko, F. A study of cytokines in burn blister fluid related to wound healing. *Burns* **21:** 352, 1995.
37. Robertson, J. G., Pickering, K. J., and Belford, D. A. Insulin-like growth factor I (IGF-I) and IGF-binding proteins in rat wound fluid. *Endocrinology* **137:** 2774, 1996.
38. Grayson, L. S., Hansbrough, J. F., Zapata-Sirvent, R. L., Dore, C. A., Morgan, J. L., and Nicolson, M. A. Quantitation of cytokine levels in skin graft donor site wound fluid. *Burns* **19:** 401, 1993.
39. Sarber, R., Hull, B., Merrill, C., Soranno, T., and Bell, E. Regulation of proliferation of fibroblasts of low and high population doubling levels grown in collagen lattices. *Mech. Ageing Dev.* **17:** 107, 1981.
40. Alberts, B., Bray, D., Lewis, J., Raff, M., Roberts, K., and Watson, J. D. *Molecular Biology of the Cell*, 3rd ed., New York: Garland, 1994.
41. Schmitt-Graff, A., Desmouliere, A., and Gabbiani, G. Heterogeneity of myofibroblast phenotypic features: An example of fibroblastic cell plasticity. *Virchows Arch.* **425:** 3, 1994.
42. Desmouliere, A., and Gabbiani, G. The role of the myofibroblast in wound healing and fibrocontractive diseases. In R. A. F. Clark (Ed.), *The Molecular and Cellular Biology of Wound Repair*. New York: Plenum, 1996. Pp. 391–423.
43. Desmouliere, A., Rubbia-Brandt, L., Abdiu, A., Walz, T., Macieira-Coelho, A., and Gabbiani, G. Alpha-smooth muscle actin is expressed in a subpopulation of cultured and cloned fibroblasts and is modulated by gamma-interferon. *Exp. Cell Res.* **201:** 64, 1992.
44. Arora, P. D., Narani, N., and McCulloch, C. A. The compliance of collagen gels regulates transforming growth factor-beta induction of alpha-smooth muscle actin in fibroblasts. *Am. J. Pathol.* **154:** 871, 1999.
45. Harris, A. K., Stopak, D., and Wild, P. Fibroblast traction as a mechanism for collagen morphogenesis. *Nature* **290:** 249, 1981.
46. Heldin, C.-H., and Westermark, B. Platelet-derived growth factor: Mechanism of action and possible in vivo function. *Cell Regul.* **1:** 555, 1990.
47. Holund, B., Junker, P., Garbarsch, C., Christoffersen, P., and Lorenzen, I. Formation of granulation tissue in subcutaneously implanted sponges in rats. A comparison between granulation tissue developed in viscose cellulose sponges (Visella) and in polyvinyl alcohol sponges (Ivalon). *Acta Pathol. Microbiol. Scand. [A]* **87A:** 367, 1979.
48. Halliday, N. L., and Tomasek, J. J. Mechanical properties of the extracellular matrix influence fibronectin fibril assembly in vitro. *Exp. Cell Res.* **217:** 109, 1995, doi: 10.1006/excr.1995.1069.
49. Mochitate, K., Pawelek, P., and Grinnell, F. Stress relaxation of contracted collagen gels: Disruption of actin filament bundles, release of cell surface fibronectin, and down-regulation of DNA and protein synthesis. *Exp. Cell Res.* **193,** 198, 1991.
50. Grinnell, F. Fibroblast–collagen-matrix contraction: Growth-factor signaling and mechanical loading. *Trends Cell Biol.* **10:** 362, 2000.
51. Maheshwari, G., Wells, A., Griffith, L. G., and Lauffenburger, D. A. Biophysical integration of effects of epidermal growth factor and fibronectin on fibroblast migration. *Biophys. J.* **76:** 2814, 1999.
52. Ware, M. F., Wells, A., and Lauffenburger, D. A. Epidermal growth factor alters fibroblast migration speed and directional persistence reciprocally and in a matrix-dependent manner. *J. Cell Sci.* **111:** 2423, 1998.
53. Barocas, V. H., Girton, T. S., and Tranquillo, R. T. Engineered alignment in media equivalents: Magnetic prealignment and mandrel compaction. *J. Biomech. Eng.* **120:** 660, 1998.
54. Mignatti, P., Rifkin, D. B., Welgus, H. G., and Parks, W. C. Proteinases and tissue remodeling. In R. A. F. Clark (Ed.), *The Molecular and Cellular Biology of Wound Repair*. New York: Plenum, 1996. Pp. 427–474.
55. Madri, J. A., Pratt, B. M., and Tucker, A. M. Phenotypic modulation of endothelial cells by transforming growth factor-beta depends upon the composition and organization of the extracellular matrix. *J. Cell Biol.* **106:** 1375, 1988.
56. Ikuno, Y., Leong, F. L., and Kazlauskas, A. Attenuation of experimental proliferative vitreoretinopathy by inhibiting the platelet-derived growth factor receptor. *Invest. Ophthalmol. Visual Sci.* **41:** 3107, 2000.
57. Scherer, G. W., Pardenek, S. A., and Swiatek, R. M. Viscoelasticity in silica gel. *J. Non-Cryst. Solids* **108:** 14, 1988.